Ductile fracture behavior in micro-scaled progressive forming of Magnesium-Lithium alloy sheet

Jilai WANG (jlwang@sdu.edu.cn)
Shandong University https://orcid.org/0000-0002-1010-5573
Zhifei Xiao
Xin Wang
Yan Sun
Chaoyang Sun

Research Article

Keywords: Micro-scaled progressive sheet forming, Size effect, Ductile fracture, Shear damage, GTN model

Posted Date: February 11th, 2022

DOI: https://doi.org/10.21203/rs.3.rs-1332234/v1

Ductile fracture behavior in micro-scaled progressive forming of Magnesium-Lithium alloy sheet

Jilai Wang[a,b*], Zhifei Xiao[a,b], Xin Wang[a,b],Yan Sun[c,d], Chaoyang Sun[e]

[a] Key Laboratory of High Efficiency and Clean Mechanical Manufacture of Ministry of Education, School of Mechanical Engineering, Shandong University, Jinan, Shandong, 250061, China

[b] National Demonstration Center for Experimental Mechanical Engineering Education, Shandong University, Jinan, Shandong, 250061, China

[c] Institute of Laser & Optoelectronics, School of Precision Instruments and Opto-Electronics Engineering, Tianjin University, Tianjin, 300072, China

[d] Shandong Nonmetallic Materials Institute, Jinan, Shandong, 250031, China

[e] Beijing Key Laboratory of Lightweight Metal Forming, School of Mechanical Engineering, University of Science and Technology Beijing, PR China

Abstract

Micro-scaled progressive sheet metal forming is a promising process for producing bulk microparts, given itsadvantages of high efficiency and low cost. To enhance forming quality andefficiency, it is important to have an in-depth understanding of the forming mechanism andmodel the forming process and fracture behavior accurately. However, prediction of fracture formation in sheet materials at the micro scale has not yet been well explored, and thus current knowledgeis not sufficient to support the continued development and application of microforming technology. This study investigated progressive sheet forming of magnesium–lithium alloy sheets of different grain sizes to produce bulk microparts directly from sheet metal via shearing, extruding, piercing, and blanking. Using the Gurson–Tvergaard–Needleman (GTN) damage model, the effects of the size factor on the formation and evolution of voids were considered, and the shear-modified GTN model was established by combining Thomason's and Lemaitre's damage mechanics models. The modified model could predict not only the ductile fracture behavior dominated by tension under high stress triaxiality at the micro scale, but also the damage behavior controlled by shear deformation under low stress triaxiality. The progressive forming process was simulated using the modified model, which was verified by experimentation and simulation. Comparisons of the experiments and simulations revealed the size effects on the forming defects and fracture behaviors of microparts during progressive sheet forming. The results show that the stress during deformation is mainly concentrated at the edge of mircoparts, and irregular geometric defects include burr, rollover, incline, and bulge become deteriorated with the increase of the initial grain size. This study enhances the understanding and prediction of ductile fracture in the micro-scaled progressive forming of sheet metals.

Keywords: Micro-scaled progressive sheet forming; Size effect; Ductile fracture; Shear damage; GTN model

Corresponding authors:

* Jilai Wang

E-mail: jlwang@sdu.edu.cn

1. Introduction

Given the increasing demands for miniaturization in electronics, medical, precision instruments, aerospace, and mangy other industrial clusters, there is an urgent need for development of efficient micro-manufacturing processes and its tooling[1-3]. Recent flexibility improvements in metal forming through combinations of different processes have played a vital role in the manufacturing industry[4,5]. Tang et al.[6] demonstrated that progressive sheet microforming for the creation of bulk microparts is a promising process due to its advantages of low production cost and high efficiency, as well as the ability to obtain net shapes or near net shapes. Notably, the positioning, forming, and blanking of dies take the same position alignment in the micro-scaled progressive sheet forming process, which ensures the dimensional accuracy and precision of the formed parts [7].

To produce bulk meso-/micro-parts directly using sheet metal, Chan and Fu[7] proposed meso-scaled progressive forming to solve the difficulties in handling and transporting microparts during microforming, Thus, cylindrical and flanged microparts can be produced through single-stroke shearing or multi-stage shearing and extrusion operations. Using metal sheets with different grain sizes, Fu and Chan[8] further examined the feasibility of fabricating micro-scaled parts with more complex features based on the flow behavior and forming characteristics of the material. Thus, they explored size effects in micro-scaled progressive forming. According to Qiu et al.[9] during the microforming process, the forming characteristics are influenced by the size effect as the size of the part decreases.

In addition to the physical experiments described above, numerous studies have been carried out to investigate the size effect on material mechanical response in the forming process[10,11]. By conducting tensile tests of copper and aluminum alloys, Miyazaki et al.[12] concluded that flow stress decreases with reduction in specimen thickness. Chan and Fu[13] also confirmed this phenomenon via pure copper compression experiments. Simons and Weippert[14] conducted tensile tests on thin copper foils of different thicknesses and showed that fracture strain decreases as the specimen thickness reduces. Fureshima et al.[15] investigated the ductile fracture behavior of copper foils and sheets of initial thicknesses of 0.05, 0.1, 0.3, and 0.5 mm, and concluded that the ductile fracture criterion at the macroscopic scale cannot be used to predict the tensile fracture of metal foils at the micro/mesoscopic scale. Xu et al.[16] found that the deformation and fracture behavior of brass foil during the micropunching process are related not only to blanking clearance but also to grain size.

When conducting the forming process, it is important to understand the fracture mechanisms of the materials involved to support defect-free micropart design, process determination, die design, and product quality assurance[17,18]. Therefore, it is crucial to study the constitution models and ductile fracture criteria of metallic materials that form part of amicroforming processes [19,20]. Extensive research has been conducted on the ductile fractures of sheet metals, shedding light on various applicable ductile fracture criteria [21]. Among these criteria, Yildiz and Yilmaz[22] proved that the GTN model is a coupled fracture model based on void damage with a sound physical basis. The model was originally introduced by Gurson[23] and has been improved upon a number of times. Engel and Kstein[11] extended the GTN model by replacing the von Mises yield function with Hill's quadratic anisotropic yield criterion. Nielsen and Tvergaard[24] introduced an extra damage term in the void evolution law to predict damage accumulation under a wide range of triaxiality. Later, Zhou et al.[25] modified the GTN model by combining Lemaitre's damage mechanics concept with the model to represent void damage and shear damage. Xu et al.[26] made an in-depth analysis of the size effect on ductile fracture through physical experiments and established an extended GTN-Thomason model by taking account of the effects of geometric shape and grain size on micro/mesoscale plastic deformation. Recently, Chen et al.[27] extended the GTN model by considering the effects of nucleation of shear softening and localization due to existing voids, and successfully applied the extension to conduct an indentation damage simulation. Although the GTN model has been extensively developed, it is difficult to predict ductile fractures accurately under multi-stress triaxiality in micro-scaled progressive forming processes, as the model does not consider shear damage and its size effect.

In this study, a shear-modified GTN model was developed to predict the deformation and fracture behaviors in a micro-scaled progressive sheet forming process. First, a series of tensile tests of were carried out on Magnesium-lithium (Mg-Li) alloy specimens of different grain sizes and the influence of grain size and stress state on ductile fracture was analyzed. The shear-modified GTN model was proposed by adding size factor and shear damage on the basis of GTN model. Finally, the shear-modified GTN model was embedded in ABAQUS to carry out finite element(FE) simulation of the progressive sheet forming process, and the obtained simulation results were compared with the corresponding experiment to verify the proposed model. Furthermore, the forming defects and fracture behaviors of the material in the progressive sheet forming process were discussed.

2. Research methodology

Based on the GTN model, a shear-modified GTN model was established by adding a shear correction term and combining it with the Thomason model to predict the deformation behavior of Mg-Li alloy in progressive sheet forming process. Uniaxial tensile tests were carried out using specimens with different grain sizes. The stress-strain curve of uniaxial tension was obtained, and the experimental results were compared with the simulation results to determine the parameters related to damage and size in the modified model. Finally, the shear-modified GTN model was used to predict the fracture and deformation behavior in progressive sheet forming process, and it was compared with the experiment to analyse the size effect on metal forming.

2.1 Modeling process

Tvergaard and Needleman[28] declared that the GTN model is a classical coupling ductile fracture criterion, which can be expressed as:

$$\Phi = \left[\frac{\bar{\sigma}}{\sigma_0(\bar{\varepsilon})}\right]^2 + 2q_1 f^*(\mathrm{f})\cosh\left[\frac{-3q_2\sigma_m}{2\sigma_0(\bar{\varepsilon})}\right] - (1 + q_3\left[f^*(f)\right]^2) = 0 \tag{1}$$

where, $\bar{\sigma}$ is the von mises equivalent stress, $\sigma_{\mathrm{m}} = \frac{1}{3}\sigma_{kk}$ is the hydrostatic stress, σ_0 is the equivalent stress of the base material, q_1 q_2 and q_3 are the coefficients. f^* is the effective void volume fraction and defined as:

$$f^* = \begin{cases} f & f < f_c \\ f_c + \dfrac{f_u - f_c}{f_f - f_c}(f - f_c) & f \geq f_c \end{cases} \tag{2}$$

Where, f_c is the critical void volume fraction onset of void coalescence. $\frac{f_u - f_c}{f_f - f_c}$ is employed to describe the fast loss of load capability. $f_u = \frac{1}{q_1}$ is the void volume fraction at which the stress of the material equals zero. f_f is the final void volume fraction when a failure occurs.

The plastic flow of the metal material is related to the cumulative plastic strain $\bar{\varepsilon}_m^{pl}$ and void volume fraction f of the matrix material. The evolution equation of equivalent plastic strain of matrix material can be obtained from the equivalent plastic work principle.

$$(1-f)\sigma_m d\bar{\varepsilon}_m^{pl} = \sigma : d\varepsilon^p \tag{3}$$

Where, $\bar{\varepsilon}_m^{pl}$ is the cumulative equivalent plastic strain increment of the matrix material, ε^p is macroscopic plastic strain increment.

2.1.1 The evolution process of void

The evolution process of void in the GTN model consists of two parts, namely the nucleation process of void and the void growth process under hydrostatic stress. The void increment expression is:

$$df = df_{growth} + df_{nucleation} \tag{4}$$

Void growth is based on bulk material incompressibility under plastic deformation, void growth is only related to the hydrostatic component of macroscopic plastic strain.

$$df_{growth} = (1-f)d\varepsilon_{kk} \tag{5}$$

Where $d\varepsilon_{kk}$ is the spheroidal portion of the strain rate.

Xu et al.[26] explored that the grain size and geometry size have an effect on the number of void nucleation using micro-scaled uniaxial tensile experiments. During the forming process, the void tends to nucleate at the internal grain boundary, but the nucleation of the void rarely occurs in the surface layer[29]. As shown in Fig. 1, when *t/d* (*t*: thickness of sheet, *d*: grain size) decreases, the surface grains occupy a larger proportion and the so-called " nucleation zone" becomes smaller. Considering the influence of size effect on the void nucleation, a size factor was added to the void nucleation model and modified to:

$$\begin{cases} df_{nucleation} = Ad\bar{\varepsilon}_M \\ A = \dfrac{\left(1-\dfrac{d}{t}\right)f_N}{S_N\sqrt{2\pi}}\exp\left(-\dfrac{1}{2}\left(\dfrac{\bar{\varepsilon}_M-\varepsilon_N}{S_N}\right)^2\right) \end{cases} \tag{6}$$

Where, ε_N S_N f_N is the material constant of the void nucleation model, $\bar{\varepsilon}_M$ is the mean equivalent plastic strain for nucleation. $1-\frac{d}{t}$ is size factor of material, which represents that with the increase of grain size, nucleation becomes more difficult.

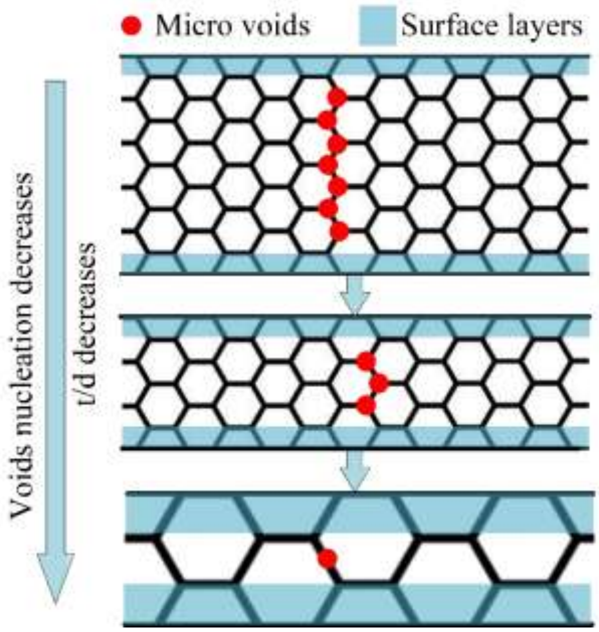

Fig. 1. Schematic diagram of the size effect on voids nucleation [26].

2.1.2 Plastic behavior of the matrix material

The matrix material of the specimen is affected by the size effect. A large number of studies have shown that in microforming of metallic alloys, the size effect is characterized by material geometry (plate thickness: *t* or cylindrical diameter: *D*) and grain size (*d*), on which the surface layer model is proposed[30]. The surface layer model is a semi-theoretical model as shown below:

$$\begin{cases} \sigma = \eta\sigma_s + (1-\eta)\sigma_i \\ \eta = \dfrac{N_s}{N} \end{cases} \tag{7}$$

Where, σ_s is the flow stress of the external grain, σ_i is the internal grain flow stress, N_s is the number of surface grains, N is the grain number of the specimen. In micro/mesoscopic scale, the effect of surface grains becomes more significant with the increase of η.

Based on the surface layer model, Peng et al.[31] proposed a constitutive model considering the size effect: since the surface grains are almost unconstrained, which are treated as single crystals, while the internal grains are treated as polycrystals. Lai et al.[32] presented that the surface grain stress can be expressed in terms of crystal plasticity theory using the Hall-Petch equation for internal grain stress.

$$\begin{cases} \sigma_s(\bar{\varepsilon}) = m\tau_R(\bar{\varepsilon}) \\ \sigma_i(\bar{\varepsilon}) = M\tau_R(\bar{\varepsilon}) + \dfrac{k(\bar{\varepsilon})}{\sqrt{d}} \end{cases} \tag{8}$$

Where, m and M are crystal direction factors of single crystal and polycrystal respectively. $\tau_R(\bar{\varepsilon})$ is the principal decomposition shear stress of a single grain, $k(\bar{\varepsilon})$ is the resistance stress of the grain boundary, and d is the grain size. For sheet metal, the proportion of surface layer grains in the material is calculated by following equation:

$$\eta = \frac{N_s}{N} = \frac{wt - [(w-2d)(t-2d)]}{wt} = \frac{2d}{t} + \frac{2d}{w} - \frac{4d^2}{wt} \tag{9}$$

Where w and t are the width and thickness of the sheet respectively. In the microforming process, w is usually much larger than t and d, so the size factor can be simplified to:

$$\eta = \frac{N_s}{N} \approx \frac{2d}{t} \tag{10}$$

2.1.3 Void coalescence

The void coalescence was determined by the Thomason model. Thomason [33] assumes that void begins to gather when stress concentration occurs in the void gap. As shown in Fig. 2, the material is treated as a regular cylindrical unit with a height of $2H$, a width of $2L$, and a spherical void of $2R$ in diameter. $\chi = \frac{R}{L}$ is the ratio of void diameter to cell width. As χ approaches 1, the void begins to coalescence. According to Benzerga et al.[34] and Besson[35] χ can be expressed as:

$$\chi = (\frac{3}{2} f \lambda_0 (\frac{3}{2} k e_{zz}))^{1/3} \tag{11}$$

Where，e_{zz} is the maximum principal strain, k is a fitting parameter used to represent material characteristics, and generally equals 1. Pardoen and Hutchinson[36] pointed that $\lambda_0 = \frac{H}{L}$ represents the spatial distribution of the void, and λ_0 is the most influential parameter in the process of void aggregation. Since the distribution of void is closely related to grain size and geometrical size, the height H and width L of the element body need to be discussed in combination with the size effect. During sheet metal forming, the thickness is much smaller than the dimensions in other two directions, and the fracture always occurs in the direction of thickness, so L is in the direction of thickness and H is in the direction of main stress. The cell height H increases with the increase of grain size. Assume that H is proportional to the average diameter of the grain, which is $2H = C_1 d$. On the other hand, with the increase of the size factor, the grains in the thickness direction decrease and the formation of voids decreases. So L is the thickness of the inner layer divided by the number of voids, which is $2L = (t-d)/N$, Where N depends on void nucleation:

$$\begin{cases} N = \int A' d\bar{\varepsilon}_M dt = \int \frac{(1-d/t) f_0}{S_N \sqrt{2\pi}} e^{(-\frac{1}{2}\frac{\bar{\varepsilon}_M - \varepsilon_N}{S_N})^2} d\bar{\varepsilon}_M = C_2 (t-d) \rho(d\bar{\varepsilon}_M) \\ \rho(d\bar{\varepsilon}_M) = \int \frac{\rho_0}{S_N \sqrt{2\pi}} e^{(-\frac{1}{2}\frac{\bar{\varepsilon}_M - \varepsilon_N}{S_N})^2} d\bar{\varepsilon}_M \approx \dfrac{e^{\frac{4}{S_N\sqrt{2\pi}}(\bar{\varepsilon}_M - \varepsilon_N)}}{1 + e^{\frac{4}{S_N\sqrt{2\pi}}(\bar{\varepsilon}_M - \varepsilon_N)}} \end{cases} \tag{12}$$

Where $C_2 = N_0 t / \rho_0$ is a constant associated with the material. Therefore, λ_0 can be expressed as:

$$\lambda_0 = \frac{H}{L} = \frac{C_1 d C_2 (t-d) \rho(d\bar{\varepsilon}_M)}{(t-d)} = C d \rho(d\bar{\varepsilon}_M) \tag{13}$$

Where $C = C_1 C_2$ is a constant associated with the material.

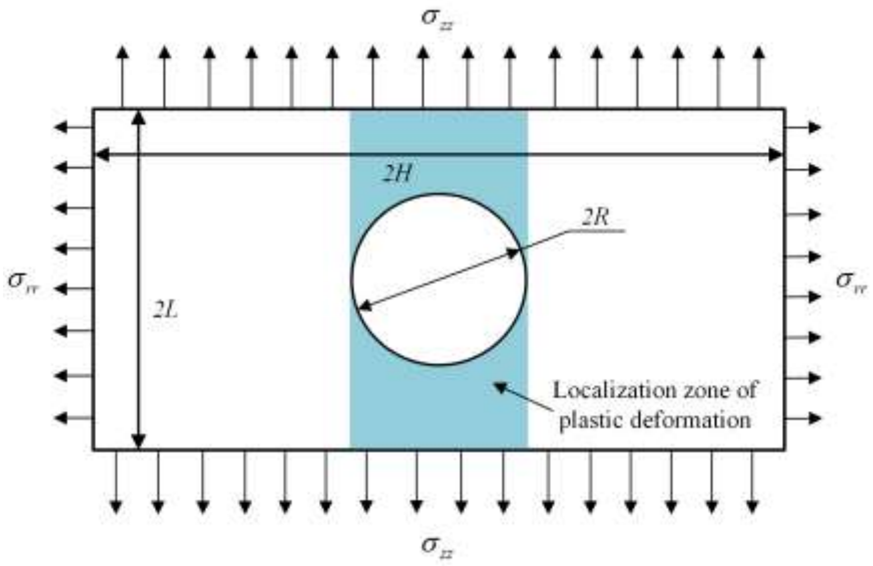

Fig. 2. Thomason model of spherical voids.

2.1.4 Modeling process considering the shear effect

The specimens were scanned by SEM and it was found that the fractured surfaces caused by different stress states had different morphological fractures[37,38] Under high stress triaxiality, the fractured surfaces were covered with large and deep dimples, suggesting that growth and internal necking of voids being the governing rupture mechanism. Under low triaxiality the fractured surfaces were covered with elongated small shear dimples, suggesting internal void shearing being the governing rupture mechanism[39]. Li et al.[40] confirmed that while the GTN model can accurately predict the ductile fracture with high stress triaxiality, it cannot be applied to predict the strain localization and ductile fracture with low stress triaxiality and shear load, because it cannot reflect the void expansion and damage under shear load. In order to predict ductile fracture of complex stresses address the limitations of these models, Zhou et al.[25] established a modified GTN model by introducing Lemaitre's concept of damage mechanics into the void growth mode. Because of its geometrical and physical significance, the model incorporating the shear damage mechanism is expressed as:

$$\begin{cases} \Phi = \left[\dfrac{\bar{\sigma}}{\sigma_0(\bar{\varepsilon})}\right]^2 + 2q_1 f^*(\mathrm{f})\cosh\left[\dfrac{-3q_2\sigma_m}{2\sigma_0(\bar{\varepsilon})}\right] - \left[1 + \left[q_1 f^*(f) + D_s\right]^2 - 2D_s\right] = 0 \\ D = q_1 f^*(f) + D_s \\ D_s = \left(\dfrac{\bar{\varepsilon}_M}{\varepsilon_f^s}\right)^n \end{cases} \tag{14}$$

Where, ε_f^s is the fracture strain in the pure shear state, $\bar{\varepsilon}_M$ is the matrix equivalent plastic strain, and n is a weakening index greater than 1. When $\bar{\varepsilon}_M$ becomes ε_f^s, D_s equals to 1. When the total damage D reaches 1, the bearing capacity of the material is lost and fracture occurs. When there is no shear damage $D_s = 0$, the modified model is consistent with the original GTN model. When the material is in a pure shear state, the modified model is in the form of the Lemaitre model. The modified model is divided into two damage mechanisms, separating volume damage from shear damage. The new damage parameter D_s will increase under deviatoric stress, while $f^*(f)$ will increase under hydrostatic stress. Fig. 3 illustrates the yield surface on the p - q plane at different damage levels. It can be seen that the yield surface gradually shrinks to a point as $q_1 f^*$ and D_s accumulate individually or simultaneously.

For general ductile metals, the shear damage increases slowly under low stress triaxiality when the plastic strain is small and increases rapidly by the n - power when $\bar{\varepsilon}_M$ is close to ε_f^s, and n is usually greater than 4[41]. In order to describe fracture behavior using the model under complex stress state, the coupled stress state weight function of the shear model is needed. The established weight function dependent on the lode angle is used to calibrate different stress states in uniaxial tensile state and shear state.

$$dD_s = \psi(\theta, T)\frac{n\left(\bar{\varepsilon}_M\right)^{n-1}}{\left(\varepsilon_f^s\right)^n} d\varepsilon \tag{15}$$

The Lode angle function should be a non-zero value, and the negative triaxiality should be corrected[25]. The stress state weight factor function is corrected as follows:

$$\psi(\theta,T)=\begin{cases} g(\theta) & T>0 \\ g(\theta)(1-k)+k & T\le 0 \end{cases} \tag{16}$$

Where, k is a constant, $g(\theta)$ is the weight function of the Lode angle.

$$\begin{cases} g(\theta)=1-\dfrac{6|\theta|}{\pi} \\ \cos(3\theta+\dfrac{\pi}{2})=27\dfrac{J_3}{2\bar{\sigma}^3} \\ J_3=(\sigma_1-\sigma_m)(\sigma_2-\sigma_m)(\sigma_3-\sigma_m)=s_1 s_2 s_3 \end{cases} \tag{17}$$

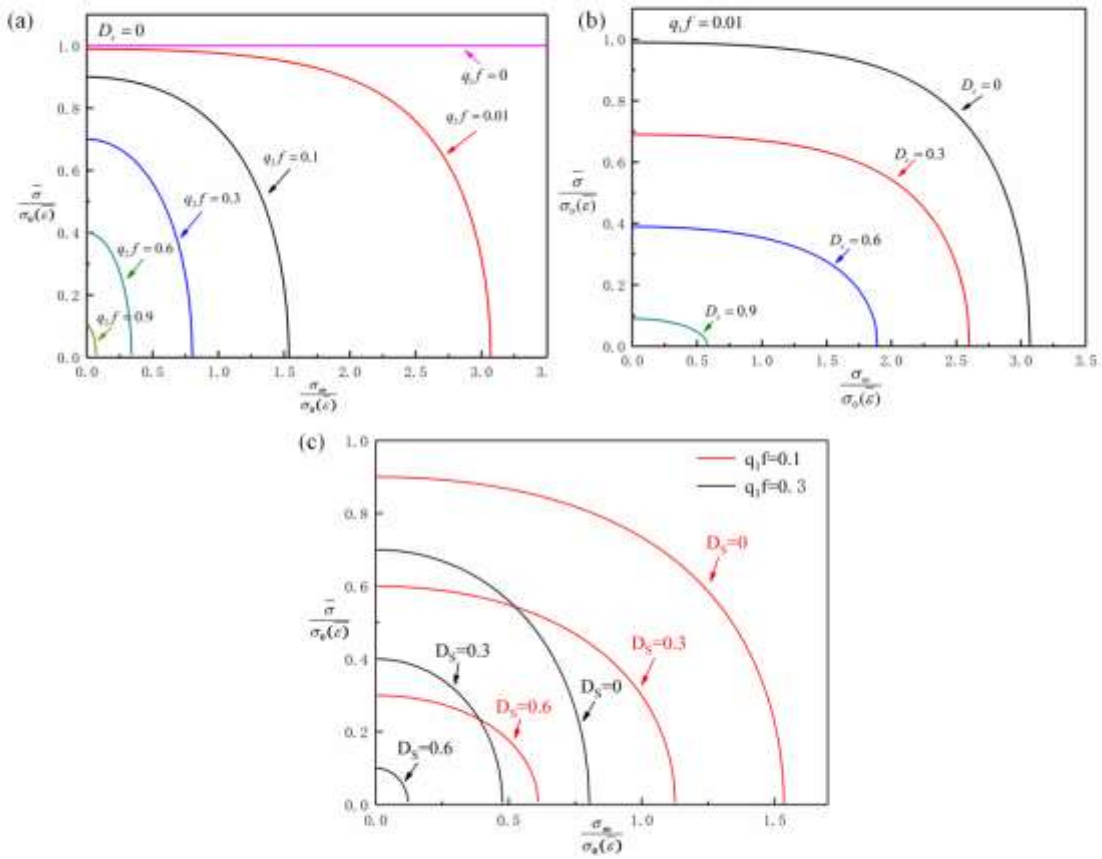

Fig. 3. Yield surface under different conditions.

2.2 Materials and experiment

In order to verify the accuracy of the shear-modified GTN model, the experiments of micro-gear progressive forming were carried out. In order to obtain the property parameters of the material, uniaxial tensile tests were carried out before the progressive forming experiments.

2.2.1 Specimen preparation

Mg-Li alloys have broad application prospects in many domains due to the unique characteristics of high strength-to-weight ratio, high dimensional stability, high specific stiffness, and good machining property. The Mg-Li alloy sheet metal with a thickness of 1 mm was chosen as the experimental material.

In this paper, the specimens were annealed at 220°C for 2 hours, 300°C for 2 hours, and 350°C for 2 hours and argon was chosen as the shielding gas. The annealing conditions for the material and the resulted average grain sizes are listed in Table 1. Grain size measured by Nano Measurer software, and the microstructure after annealing is shown in Fig. 4.

Table 1 Specimen annealing conditions and the measured grain sizes.

No.	Temperature	Duration	Grain size	Grain size deviation
1	As received		2.2 μm	0.8 μm
2	220°C	2h	8.07 μm	1.4 μm
3	300°C	2h	14.01 μm	2.1 μm
4	350°C	2h	25.5 μm	3.2 μm

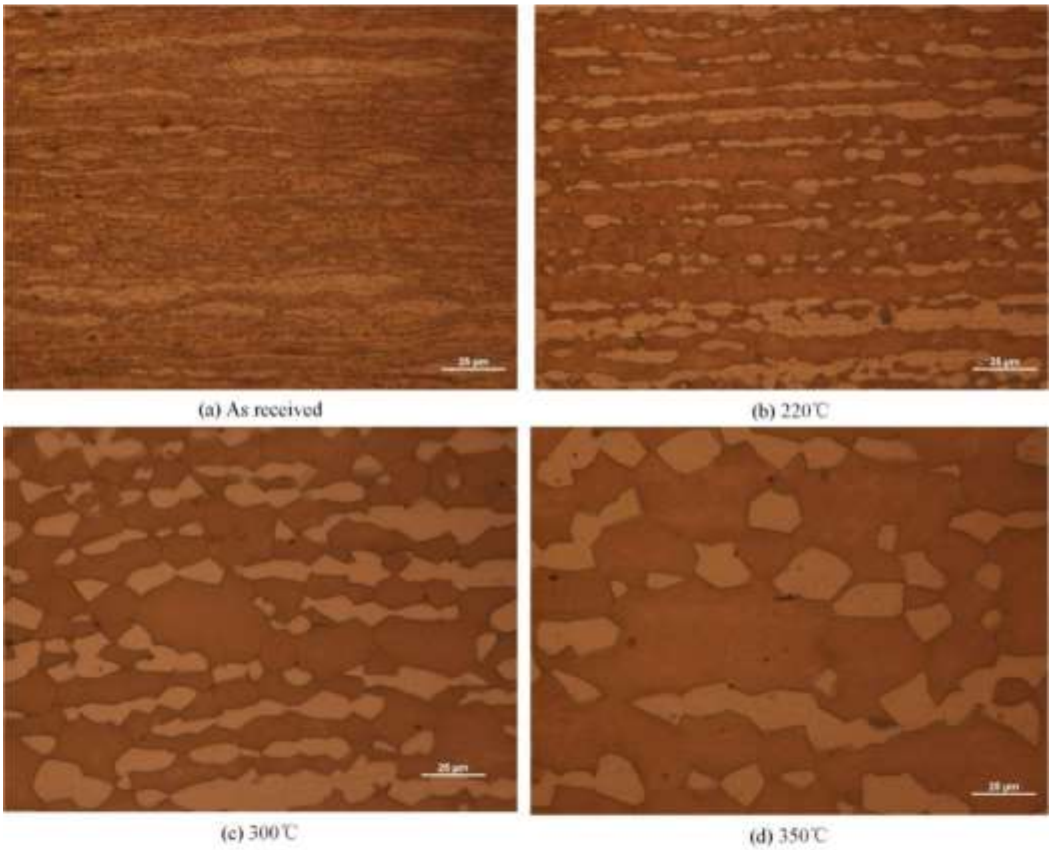

Fig. 4. Microstructures of the Mg-Li alloy in the sheet plane; (a). As-received, (b). 220°C, (c). 300 °C, and (d). 350°C.

2.2.2 Tensile tests

The specimen of tensile tests are shown in Fig. 5. Any tiny surface damage will affect the grain size effect on the material fracture behavior , therefore, all specimens were cutted by electric discharge machining. The test environment was room temperature. The instrument used is an MTS platform with a data acquisition system, a 50 KN loadcell and an extensometer. The testing speed was set to 0.01mm/s.

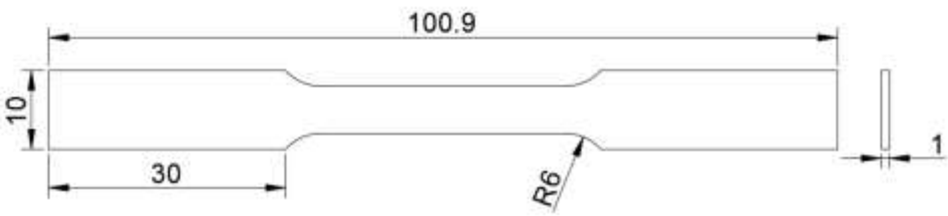

Fig. 5. Dimensions of the dog-bone shaped tensile specimen (Unit: mm).

2.2.3 Micro-scaled progressive sheet forming experiments

A set of progressive forming dies for micropart machining was developed, as shown in Fig. 6. The whole process needs three steps but the tooling does not need change. In the first step, the movement displacement of the punch is 2 mm to produce a gear profile. In the second step, on the basis of the first step, the downward displacement continues to form the flanged features on the gear parts. In the third step, the punch moves with a displacement of 1.5 mm to get the microformed gear part and the drop material produces a micro-pin.

The developed progressive microforming system was fabricated with high-speed steel. The experiment was performed on a programmable MTS tester with a maximum pressure of 50 kN. To minimize the frictional effect, machine oil was used to lubricate the interface between the die and workpiece. In order to simulate quasi-static forming, the forming speed was set to 0.01mm/s. The progressively microformed gear parts and their dimensions are shown in Fig. 7.

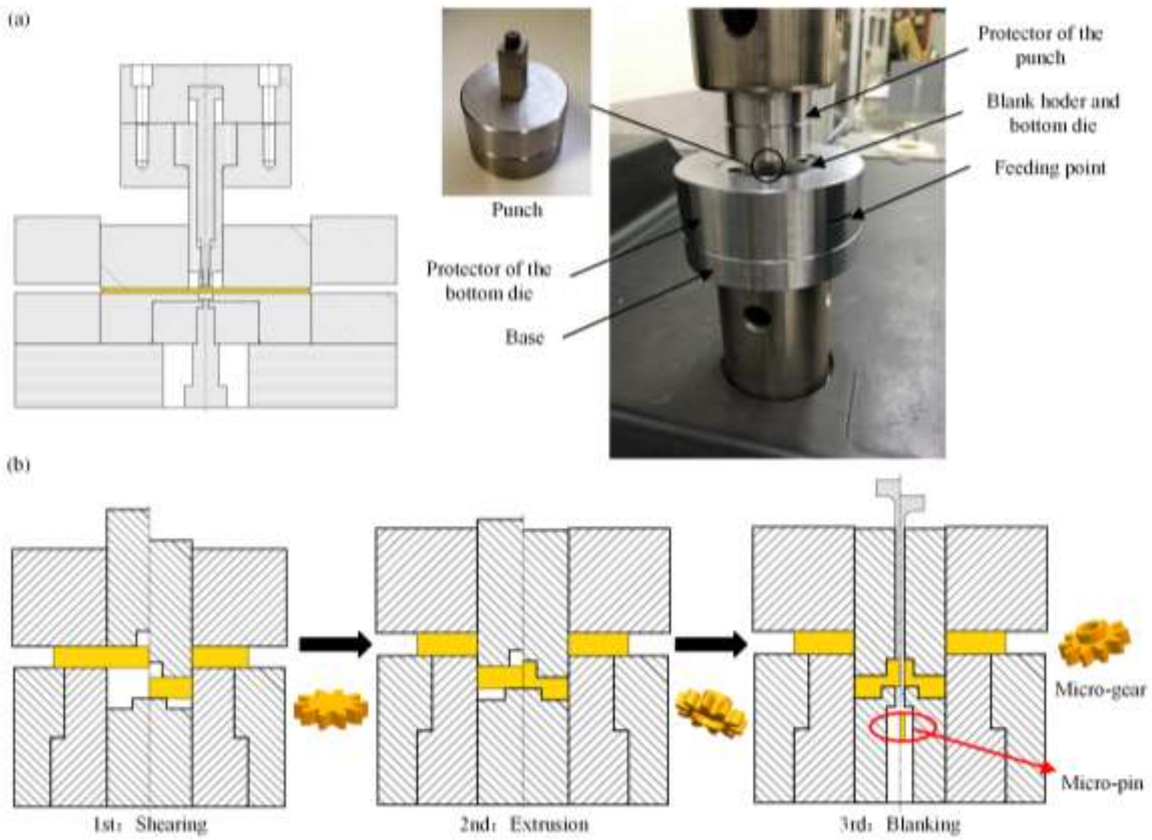

Fig. 6. Experimental configuration.

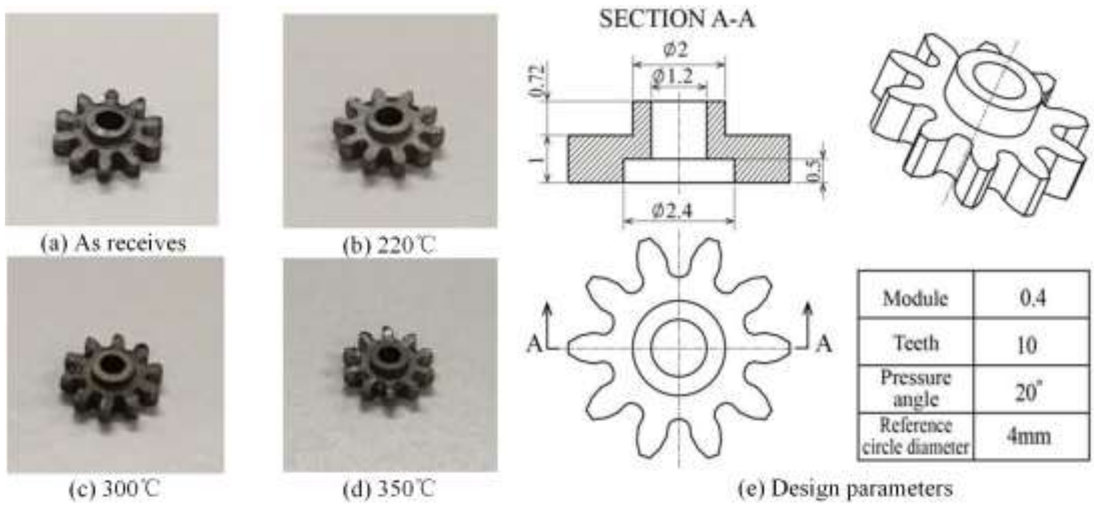

Fig. 7. Design parameters for the gear.

3. Numerical analysis and discussion

3.1 parameter determination

The true stress-strain curve is obtained through the uniaxial tensile test, and the results are shown in Fig. 8. It can be found that the flow stress decreases with the increase of grain size. According to Peng[31], for the metal in FCC lattice, m and M in the surface layer model are taken as 2 and 3.06, respectively. For other parameters in the surface layer model, the least square method is adopted to fit. $k(\bar{\varepsilon})$ and $\tau_R(\bar{\varepsilon})$ are obtained as following:

$$\begin{cases} k(\bar{\varepsilon}) = k_1(\bar{\varepsilon})^{n_1} + b \\ \tau_R(\bar{\varepsilon}) = k_2(\bar{\varepsilon})^{n_2} \end{cases} \tag{18}$$

The stress and strain equations of each d were obtained by using the swift equation fitting, and then the stress and surface grain proportion were obtained by fixing the strain. The final expressions with strain are fitted. The surface layer constitutive relationship can be expressed as:

$$\begin{cases} \sigma = \eta\left[2(14.7 + 156.75\varepsilon^{0.405})\right] \\ +(1-\eta)\left[3.06(14.7 + 156.75\varepsilon^{0.405}) + \dfrac{190.27\varepsilon^{0.0421}}{\sqrt{d}}\right] \\ \eta = \dfrac{2d}{t} \end{cases} \tag{19}$$

The material parameters in the shear-modified GTN model are shown in Table 2. In this model, q_1 and q_2 are related coefficients introduced into the GTN model by Tvergaard to better fit experimental data, which represent the void interaction. In general, q_1=1.5, q_2=1, and q_3 =2.25[42]. According to Benseddiq and Imad[43], the insignificant influence factors f_0 and S_N can be evaluated according to experience, respectively: $f_0 = 0.001$ and $S_N = 0.1$. χ_c is a critical value close to 1, indicating that the spacing of void becomes very small and microcracks form. According to Xu et al.[26], $\chi_c = 0.9$ is used in this paper to determine the void gathering. ε_N represents the moment when the void nucleates at the highest rate during the deformation process. If the void nucleation is normally distributed in the uniaxial tensile test, then the intermediate strain of the stress-strain curve can be expressed as ε_N. Through the experimental simulation comparison of the third step of progressive sheet forming process, the results are obtained by the inverse method k=0.5, ε_f^s=0.6 , and n=5[25]. Ramazani et al.[44] pointed that C , f_n and $f_f - f_c$ can be determined by trial and error method based on the stress-strain curves of uniaxial tension test.

Table 2 The parameters of the shear-modified GTN model.

ε_N	s_N	f_0	q_1	q_2	q_3	χ_c	f_n	C	$f_f - f_c$	ε_f^s	n	k
0.3	0.1	0.001	1.5	1	2.25	0.9	0.1	0.522	0.113	0.5	5	0.5

3.2 FE simulation

Shear-modified GTN model was imported into ABAQUS VUMAT user subroutine using Fortran language for simulation calculations. In ABAQUS, the model is meshed using the C3D8R type, namely 8-node linear cells. User-defined material parameters were set according to the calibrated parameters, and then determine explicit analysis steps by experimental motion speed to ensure a quasi-static process. In the simulation of forming process, 1/4 calculation is adopted to improve the operation efficiency.

3.3 Results and discussion

3.3.1 Validation of the mechanism-based constitutive model

Fig. 8 shows the true stress-strain curve of Mg-Li alloy with different grain sizes under uniaxial tension. It can be seen that the true stress slowly increase until it reaches the peak, and then the curve decreases sharply, which means that the tensile process has ended and the Mg-Li alloy was fractured. It is found that the flow stress of materials gradually decreases with the increase of grain size, and the plasticity becomes worse. The decrease of flow stress can be explained by the surface layer model. The smaller the size factor t/d, the more surface grains, and the smaller the material flow stress. The plastic variation of the material can be explained by the

Thomason model. The larger the grain, the easier the pores are to aggregate. The plasticity of untreated materials is bad because of the irregular internal grains affected by the former processing.

Uniaxial tensile tests and forming experiments with different size factors were simulated by ABAQUS/Explicit. The ture tress-strain curves from FE simulation are shown in Fig. 8. By comparison, it can be found that the shear-modified GTN model can accurately simulate the mechanical properties of materials. Uniaxial tensile test results showed that the fracture strain of 22.5μm grain size specimen was greater than 14.01 μm grain size specimen, because the number of void nucleation decreased with the increase of grain size. The evolution of f and χ is obtained and presented in Fig. 9 for the specimens with the different grain sizes. When χ reaches 0.9, the holes begin to gather, and then the specimen is necked.

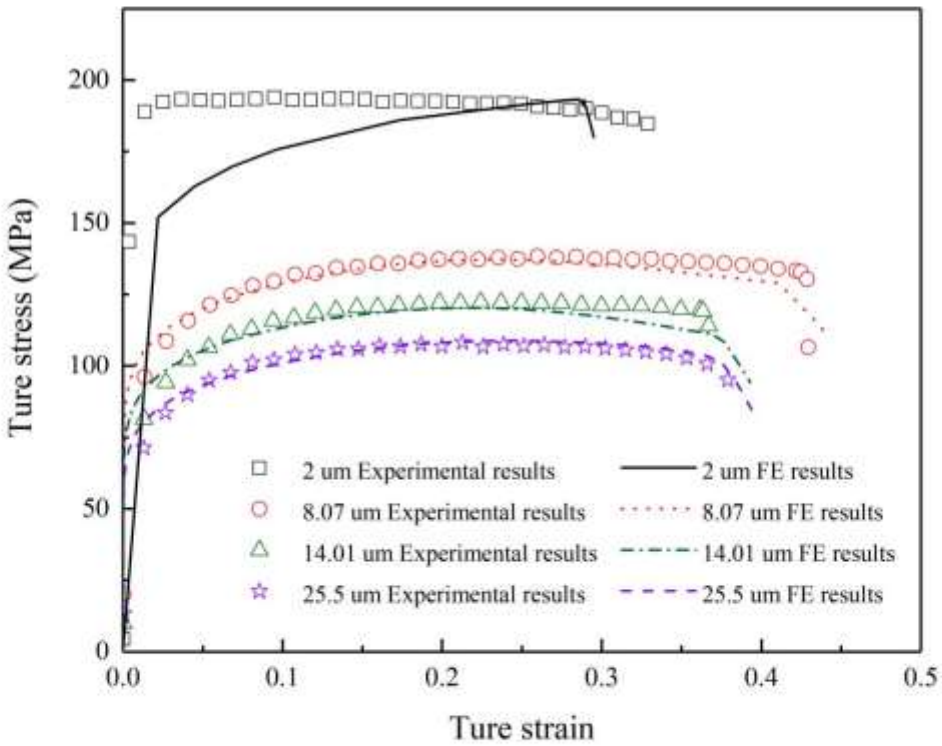

Fig. 8. Comparison of flow stresses between simulation and the experimental results.

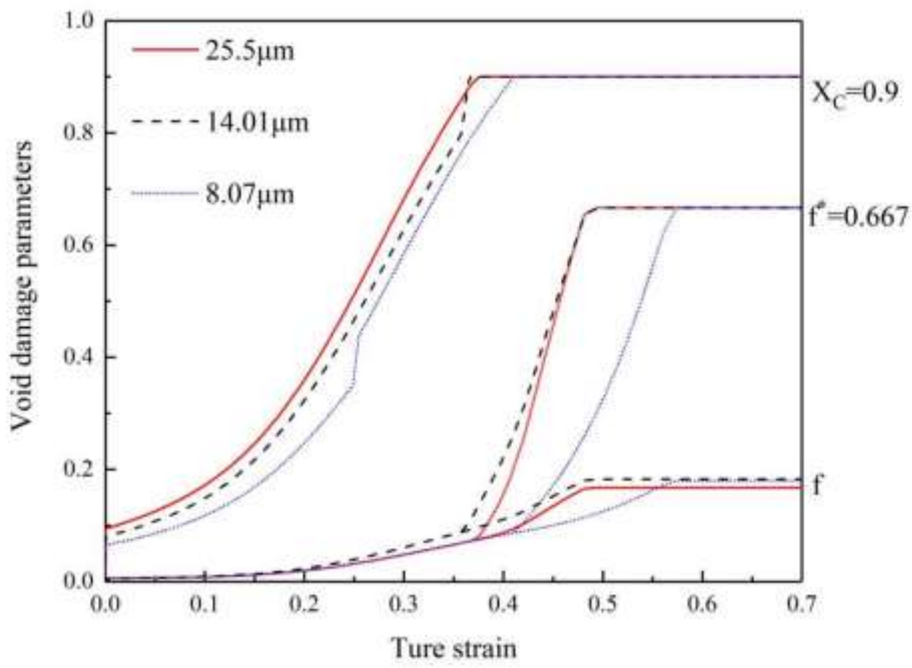

Fig. 9. The evolution of a void during a deformation.

As shown in Fig. 10, it can be found that lode function under uniaxial tension is close to 0. In the first and third steps of the experiment, the lode function formed by fracture is approximately 1. Thus it can be proved that it is feasible to use the lode function to represent the stress state. At the same time, It is found that the stress state of the specimen is always changing during the forming process. Fig. 11 shows the damage accumulation under two different fracture mechanisms, the material breaks when the total damage reaches 1. The tensile fracture is mainly caused by void-induced damage, while the shear fracture is mainly caused by shear-induced damage. Shear damage in the tensile fracture is caused by shear deformation due to stress concentration induced by necking, while void-induced damage in the shear fracture is caused by small tensile deformation at the beginning of deformation. All fracture behaviors are affected by shear- and void-induced damage, which verifies the authenticity of the shear-modified GTN model.

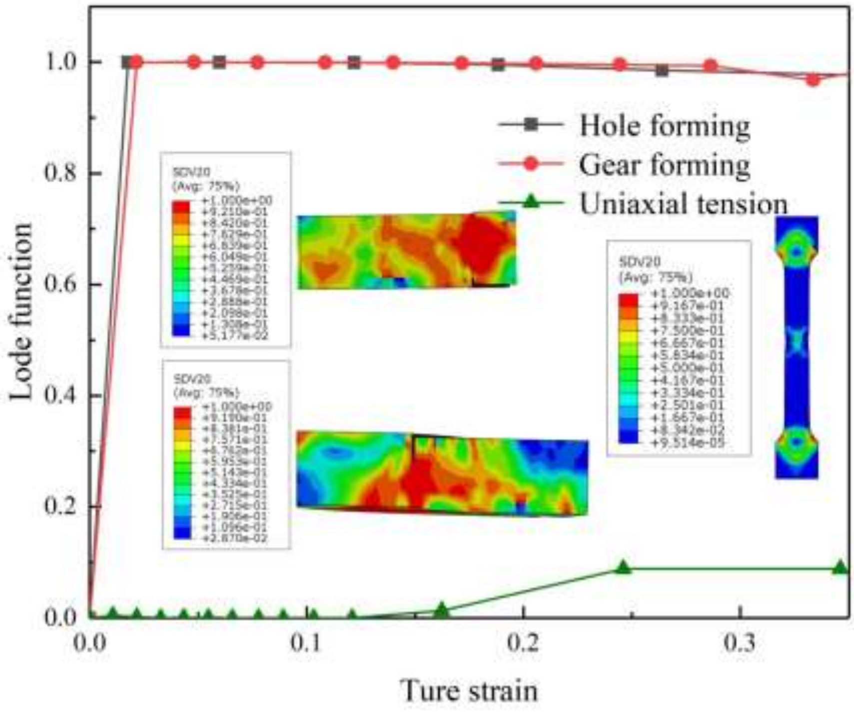

Fig. 10. Lode parameters under different stress states.

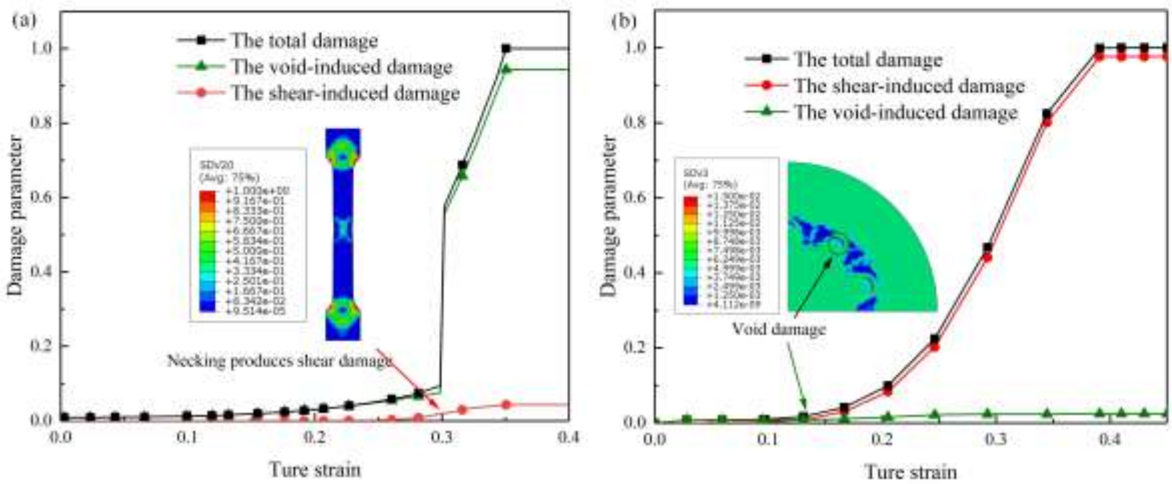

Fig. 11. The accumulation of damage during deformation.

3.3.2 Deformation behavior and microstructure

Micropins and microgears were fabricated in this research by using the progressive microforming process as shown in Fig. 6. The microgear was produced by the first stamping, and the cylindrical micropin was produced by the final punching.. In this section, the geometrical dimension, microstructure, and forming defects of the micropart was experimentally examined. The modified constitutive model was used to simulate the progressive forming via FEsimulation in ABAQUS software. In microforming manufacturing processes microparts have several forming defects, including rollover, shearing, and fracture burr. Through the comparison of simulation and experiment, it was found that the shear-modified GTN model can simulate the deformation and fracture behavior of materials well as shown in Fig. 12.

Fig. 13 shows the profile and microscopic morphology of the cross-section of the fabricated micropins under different annealing conditions of Mg-Li alloy. The undulating side edge of the micropin was observed at the coarse-grained material and the geometrical asymmetry of the pin is aggravated by increasing the grain size. At the same time, with the increase of grain size, the surface roughness of the formed parts becomes worse, because the grains in the deformation zone become less, and the deformation is controlled by single crystal. As shown in Fig. 14, the flow stress of the material in the shear process decreases with increase of grain size, resulting in the intensified asymmetry of the deformed materials.

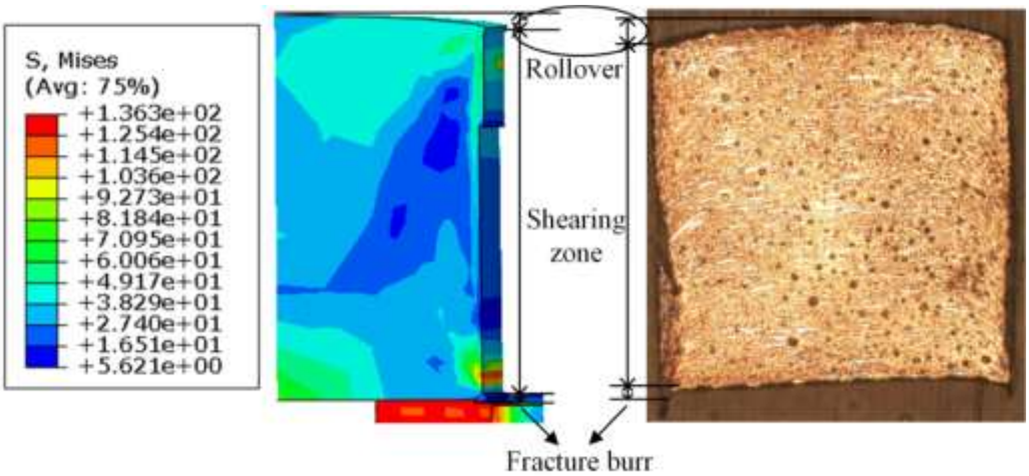

Fig. 12. Experimental and FE of cylindrical forming defects.

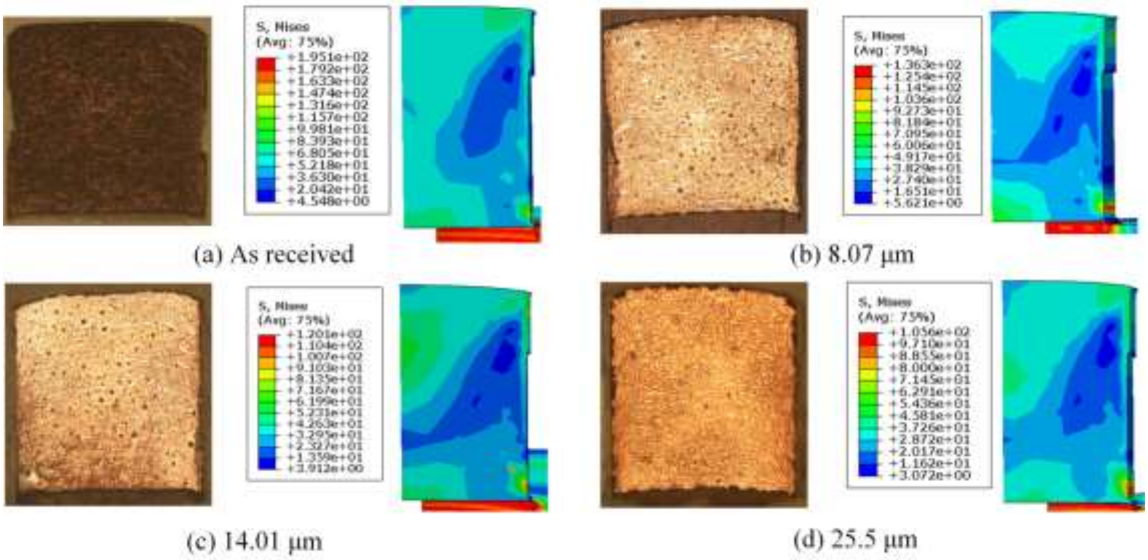

Fig. 13. Experimental and FE of micro-pin forming results.

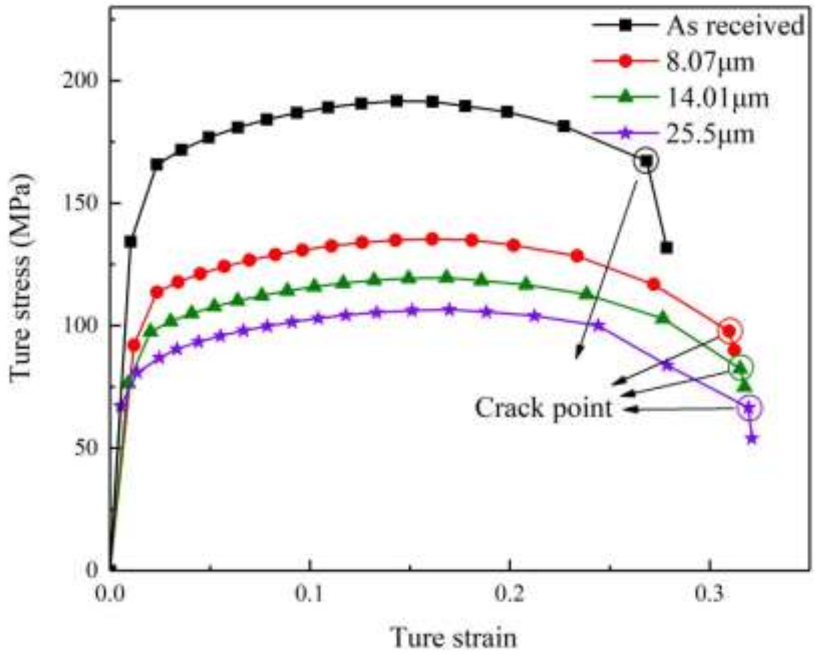

Fig. 14. Effect of grain size on fracture during micro-pin forming.

As shown in Fig. 15, it was found that the deformation during the gear forming process was mainly concentrated at the root of the tooth. The strain at the root of the tooth was also found to be the most obvious during the forming process, and the larger strain of the material, the more obvious the rollover will be, which proved that the model can well predict deformation and fracture behavior in micro-scaled progressive sheet forming process.

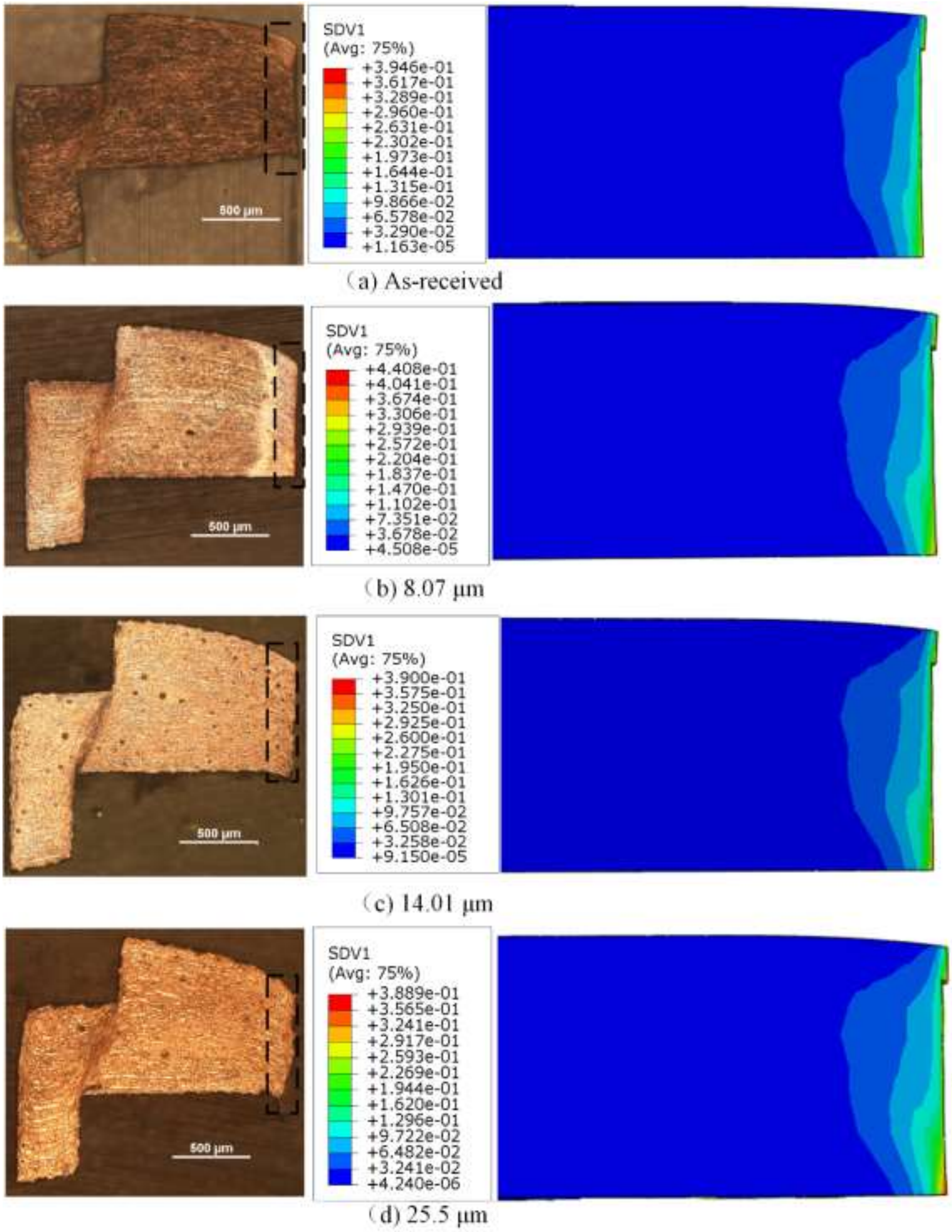

Fig. 15. Experimental and FE micro gear forming results.

In order to improve the quality of micro-scaled progressive sheet forming parts, the material flow behavior needs to be investigated. The flow pattern and geometry of the forming defects of the progressively formed micropart using the 300°C annealing treatment are shown in Fig. 16. In addition to the shear surfaces formed in the first and second steps, the material underwent severe plastic deformation in the shear band formed during the second forming step. The direction of flow of the material is shown by the arrow, the material at the left side of the shear band was pushed to zone A, whereas the right-side material flows into zone B. Due to the direction of flow of the material at an angle to the side wall of the die, this results in an incline of the forming surface. As shown in Fig. 15, the angle of incline becomes larger as the grain size increases. This is due to the fact that the influence of a single crystal on the overall flow of the material becomes more pronounced, resulting in an insufficient transverse flow of the material. The largest angle of an incline in the unannealed part is due to the presence of residual stress, resulting in insufficient material flow during deformation. It was also found that there was a bulge in the deformed part and that the bulge became more pronounced as the grain size increased. The bulge phenomenon is caused by the interface friction between the sheet metal and the die which would restrict the material flow near the interface.

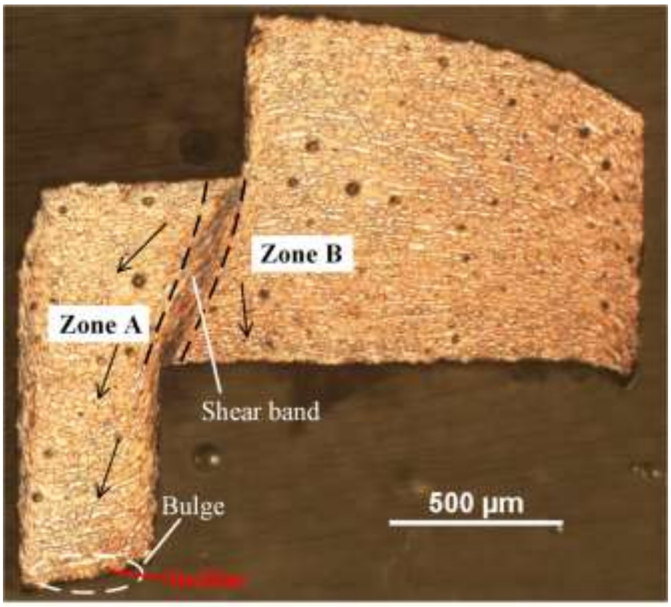

Fig. 16. Flow pattern and typical undesirable geometries of the micropart. (Black arrows

show the flow directions of the material.)

4. Conclusion

Through experiments and numerical simulation, a shear-modified GTN model was established to predict the fracture and deformation behavior in micro-scaled progressive sheet forming process. Cylindrical micro-pin and micro-gear with flange were formed by the progressive sheet forming process. The effects of grain size and stress state on the deformation behavior of Mg-Li alloy were studied from the aspects of fracture behaviors, microstructure evolution, and forming defects. The following conclusions are drawn from the present investigation:

(1) The damage accumulation in the shear-modified GTN model is induced by two independent damage parameters, respectively. The void damage is calculated by the nucleation, growth and coalescence of the void, and the shear damage is calculated in a phenomenological way with the weight function of the Lode parameter.

(2) The fracture behavior in micro-scaled progressive forming process is affected by both void- and shear-induced damage. Necking in uniaxial tensile tests could cause shear-induced fracture and void-induced damage can also be caused in shearing process.

(3) The size factor and the shear parameters are added to the GTN model to create a shear-modified model. The modified model considers not only the effect of void growth caused by hydrostatic stress on damage, but also the effect of shear stress on the damage. Finally, the accuracy of the modified model is verified by experiments.

(4) With the increase of grain size, the influence of single grain on material forming is significant. The asymmetry and unevenness of the formed surface are more serious; rollover and fracture burr are even more obvious; and the angle of the extrusion part of the incline becomes larger.

Acknowledgments

This work was supported by the Young Scholars Program of Shandong University; and the Shandong Provincial Natural Science Foundation [Grant number ZR2019BEE062].

Statements and Declarations:

The authors declare that they have no known competing financial interests or personal relationships that could have appeared to influence the work reported in this paper.

Ethics approval:

Not applicable

Consent to participate:

Not applicable

Consent for publication:

Not applicable

Availability of data and material:

Not applicable

Competing Interests:

The authors have no relevant financial or non-financial interests to disclose

Author Contributions:

All authors contributed to the study conception and design. Material preparation, data collection and analysis were performed by Jilai Wang, Zhifei Xiao and Xin Wang. The first draft of the manuscript was written by Jilai Wang and Zhifei Xiao, and all authors commented on previous versions of the manuscript. All authors read and approved the final manuscript.

References

[1] Vollertsen F, Hu Z, Niehoff HS et al (2004) State of the art in micro forming and investigations into micro deep drawing. J Mater Process Technol 151(1-3): 70-79. https://doi.org/10.1016/j.jmatprotec.2004.04.266

[2] Li QH, Sigmund O, Jensen JS, Aage N (2021) Reduced-order methods for dynamic problems in topology optimization: A comparative study. Comput Method Appl M 387:114149 https://doi.org/10.1016/j.cma.2021.114149

[3] Li QH, Wu QB, Liu J, et al (2021) Topology optimization of vibrating structures with frequency band constraints. Struct Mutidiscip O 63(3): 1203-1218. https://doi.org/10.1007/s00158-020-02753-7

[4] Yang DY, Bambach M, Cao J, et al (2018) Flexibility in metal forming. CIRP Ann-Manuf Technol 67(2). https://doi.org/10.1016/j.cirp.2018.05.004

[5] Fu MW, Wang JL, Korsunsky AM (2016) A review of geometrical and microstructural size effects in micro-scale deformation processing of metallic alloy components. Int J Mach Tools Manuf 109: 94-125. https://doi.org/10.1016/j.ijmachtools.2016.07.006

[6] Tang XF, Shi SQ, Fu MW (2019) Interactive effect of grain size and crystal structure on deformation behavior in progressive micro-scaled deformation of metallic materials. Int J Mach Tools Manuf 148: 103473.

[7] Chan WL, Fu MW (2013) Meso-scaled progressive forming of bulk cylindrical and flanged parts using sheet metal. Mater Des 43: 249-257. https://doi.org/10.1016/j.matdes.2012.07.004

[8] Fu MW, Chan WL (2013) Micro-scaled progressive forming of bulk micropart via directly using sheet metals. Mater Des 49(Aug.): 774-783. https://doi.org/10.1016/j.matdes.2013.02.045

[9] Qiu TT, Hou YK, Cao HL (2017) Review of research progress on size effect in micro-forming. Key Engineering Materials 717: 118-121. https://doi.org/10.4028/www.scientific.net/KEM.717.118

[10] Fu MW, Wang JL (2021) Size effects in multi-scale materials processing and manufacturing. Int J Mach Tools Manuf 167: 103755.

https://doi.org/10.1016/j.ijmachtools.2021.103755
[11] Engel U, Ec Kstein R (2002) Microforming—from basic research to its realization. J Mater Process Technol 125: 35-44. https://doi.org/10.1016/S0924-0136(02)00415-6
[12] Miyazaki S, Shibata K, Fujita H (1979) Effect of specimen thickness on mechanical properties of polycrystalline aggregates with various grain sizes. Acta Metallurgica 27(5): 855-862. https://doi.org/10.1016/0001-6160(79)90120-2
[13] Chan WL, Fu MW (2012) Studies of the interactive effect of specimen and grain sizes on the plastic deformation behavior in microforming. Int J Adv Manuf Technol 62(9-12): 989-1000. https://doi.org/10.1007/s00170-011-3869-2
[14] Simons G, Weippert C, Dual J et al (2006) Size effects in tensile testing of thin cold rolled and annealed Cu foils. Mater Sci EngA-Struct 416(1-2): 290-299.
https://doi.org/10.1016/j.msea.2005.10.060
[15] Furushima T, TsunezakiH, Manabe K et al (2014) Ductile fracture and free surface roughening behaviors of pure copper foils for micro/meso-scale forming. Int J Mach Tools Manuf 76(76): 34-48. https://doi.org/10.1016/j.ijmachtools.2013.10.001
[16] Xu J, Guo B, Wang CJ et al (2012) Blanking clearance and grain size effects on micro deformation behavior and fracture in micro-blanking of brass foil. Int J Mach Tools Manuf 60: 27-34. https://doi.org/10.1016/j.ijmachtools.2012.04.001
[17] Patel G, Ganesh MK, Kulkarni O (2020) Experimental and numerical investigations on forming limit curves in micro forming. Adv Mater Process Technol 12.
https://doi.org/10.1080/2374068X.2020.1793268
[18] Chang ZD, Li M, Chen J (2019) Analytical modeling and experimental validation of the forming force in several typical incremental sheet forming processes. Int J Mach Tools Manuf 140: 62-76. https://doi.org/10.1016/j.ijmachtools.2019.03.003
[19] Ahn K, Huh H, Yoon J (2015) Rate-dependent hardening model for pure titanium considering the effect of deformation twinning. Int J Mech Sci 98: 80-92.
https://doi.org/10.1016/j.ijmecsci.2015.04.008
[20] Xuan X, Wang M, Zhang M, et al (2022) Nanoarchitectonics of low-dimensional metal-organic frameworks toward photo/electrochemical CO2 reduction reactions. J CO2 UTIL 57: 101883.

https://doi.org/10.1016/j.jcou.2022.101883

[21] Lou YS, Huh H (2013) Prediction of ductile fracture for advanced high strength steel with a new criterion: Experiments and simulation. J Mater Process Technol 213(8): 1284-1302. https://doi.org/10.1016/j.jmatprotec.2013.03.001

[22] Yildiz RA, Yilmaz S (2020) Experimental Investigation of GTN model parameters of 6061 Al alloy. Eur J Mech A-Solids 83. https://doi.org/10.1016/j.euromechsol.2020.104040

[23] Gurson AL (1977) Continuum theory of ductile rupture by void nucleation and growth: Part I—Yield criteria and flow rules for porous ductile media. J Eng Mater Technol-Trans ASME 99(1): 2-15. https://doi.org/10.1115/1.3443401

[24] Nielsen KL, Tvergaard V (2010) Ductile shear failure or plug failure of spot welds modelled by modified Gurson model. Eng Fract Mech 77(7): 1031-1047. https://doi.org/10.1016/j.engfracmech.2010.02.031

[25] Zhou J, Gao XS, Sobotka JC et al (2014) On the extension of the Gurson-type porous plasticity models for prediction of ductile fracture under shear-dominated conditions. Int J Solids Struct 51(18): 3273-3291. https://doi.org/10.1016/j.ijsolstr.2014.05.028

[26] Xu ZT, Peng LF, Fu MW et al (2015) Size effect affected formability of sheet metals in micro/meso scale plastic deformation: Experiment and modeling. Int J Plast 68: 34-54. https://doi.org/10.1016/j.ijplas.2014.11.002

[27] Chen Y, Zhang C, Varé C (2017) An extended GTN model for indentation-induced damage. Comput Mater Sci 128: 229-235. https://doi.org/10.1016/j.commatsci.2016.11.043

[28] Tvergaard V, Needleman A (1984) Analysis of the cup-cone fracture in a round tensile bar. Acta Metallurgica 32(1): 157-169. https://doi.org/10.1016/0001-6160(84)90213-X

[29] Rudd RE, Belak JF (2002) Void nucleation and associated plasticity in dynamic fracture of polycrystalline copper: an atomistic simulation. Comput Mater Sci 24(1-2): 148-153. https://doi.org/10.1016/S0927-0256(02)00181-7

[30] Zhai JQ, Guan YJ, Wang WG (2020) Construction of Material Constitutive Relationship Based on Surface-Layer Model at Micro/Mesoscopic Scale. Mater Trans 61(2): 256-260. https://doi.org/10.2320/matertrans.MT-ML2019016

[31] Peng LF, Lai XM, Lee HJ et al (2009) Analysis of micro/mesoscale sheet forming process with uniform size dependent material constitutive model. Mater Sci Eng A 526(1-2): 93-99. https://doi.org/10.1016/j.msea.2009.06.061

[32] Lai XM, Peng LF, Hu P et al (2008) Material behavior modelling in micro/meso-scale forming process with considering size/scale effects. Comput Mater Sci 43(4): 1003-1009. https://doi.org/10.1016/j.commatsci.2008.02.017

[33] Thomason PF (1985) A three-dimensional model for ductile fracture by the growth and coalescence of microvoids. Acta Metallurgica 33(6): 1087-1095. https://doi.org/10.1016/0001-6160(85)90202-0

[34] Benzerga AA, Besson J, Pineau A (1999) Coalescence-controlled anisotropic ductile fracture. J Eng Mater Technol-Trans ASME 121(2): 221-229. https://doi.org/10.1115/1.2812369

[35] Besson J (2009) Damage of ductile materials deforming under multiple plastic or viscoplastic mechanisms. Int J Plast 25(11): 2204-2221. https://doi.org/10.1016/j.ijplas.2009.03.001

[36] Pardoen T, Hutchinson JW (2000) An extended model for void growth and coalescence. J Mech Phys Solids 48(12): 2467-2512. https://doi.org/10.1016/S0022-5096(00)00019-3

[37] Lou YS, Huh H, Lim S et al (2012) New ductile fracture criterion for prediction of fracture forming limit diagrams of sheet metals. Int J Solids Struct 49(25): 3605-3615. https://doi.org/10.1016/j.ijsolstr.2012.02.016

[38] Wang JL, Li CZ, Wan Y et al (2020) Size effect on the shear damage under low stress triaxiality in micro-scaled plastic deformation of metallic materials. Mater Des 196: 109107. https://doi.org/10.1016/j.matdes.2020.109107

[39] Nahshon K, Xue Z (2009) A modified Gurson model and its application to punch-out experiments. Eng Fract Mech 76(8): 997-1009. https://doi.org/10.1016/j.engfracmech.2009.01.003

[40] Li X, Chen ZH, Dong CF (2020) Size effect on the damage evolution of a modified GTN model under high/low stress triaxiality in meso-scaled plastic deformation. Mater Today Commun 101782. https://doi.org/10.1016/j.mtcomm.2020.101782

[41] Wang S, Chen ZH, Dong CF (2017) Tearing failure of ultra-thin sheet-metal involving size effect in blanking process: Analysis based on modified GTN model. Int J Mech Sci 133: 288-302. https://doi.org/10.1016/j.ijmecsci.2017.08.028

[42] Chen ZY, Dong XH (2009) The GTN damage model based on Hill'48 anisotropic yield criterion and its application in sheet metal forming. Comput Mater Sci 44(3): 0-1021. https://doi.org/10.1016/j.commatsci.2008.07.020

[43] Benseddiq N, Imad A (2008) A ductile fracture analysis using a local damage model. Int J Pressure Vessels Pip. 85(4): 219-227. https://doi.org/10.1016/j.ijpvp.2007.09.003

[44] Ramazani A, Abbasi M, Prahl U et al (2012) Failure analysis of DP600 steel during the cross-die test. Comput Mater Sci 64: 101-105.
https://doi.org/10.1016/j.commatsci.2012.01.031